

Article

Hydrogen-Assisted Thermocatalysis over Titanium Nanotube for Oxidative Desulfurization

Weiwei Tang ¹, Yue Yao ^{2,*} and Xiaoqiao Huang ^{3,*}¹ Guangzhou Maritime Institute, Guangzhou 510330, China; tangww8304@163.com² College of Chemical Engineering and Materials Science, Tianjin University of Science and Technology, 29 13th Avenue, TEDA, Tianjin 300457, China³ PetroChina Fuel Oil Company Limited Research Institute, Beijing 100195, China

* Correspondence: yueyao@tust.edu.cn (Y.Y.); liaoxy@tust.edu.cn (X.H.)

Abstract: Titanium nanotubes were hydrothermally synthesized via a two-step method for ODS (oxidative desulfurization). The catalysts' structures were characterized by XRD (X-ray diffraction), FT-IR, UV-Vis (UV-Vis diffuse reflectance spectra), NH₃-TPD, etc. The effects of O/S molar ratio and catalyst dosage, etc., were systematically investigated. The catalyst exhibited remarkable performance, so that the removal of DBT (dibenzothiophene) was nearly 100% under the optimal conditions in 10 min. Also, the catalysts could be easily reused for six consecutive cycles. The hydrogen-assisted thermocatalytic mechanism over titanium nanotubes for ODS was also studied and an effective reactant concentration (ERC) number of 70.8 was calculated.

Keywords: titanium nanotubes; hydrogen-assisted; heterogeneous catalysis; ODS



Citation: Tang, W.; Yao, Y.; Huang, X. Hydrogen-Assisted Thermocatalysis over Titanium Nanotube for Oxidative Desulfurization. *Catalysts* **2022**, *12*, 29. <https://doi.org/10.3390/catal12010029>

Academic Editor: Hyun-Seog Roh

Received: 8 December 2021

Accepted: 22 December 2021

Published: 27 December 2021

Publisher's Note: MDPI stays neutral with regard to jurisdictional claims in published maps and institutional affiliations.



Copyright: © 2021 by the authors. Licensee MDPI, Basel, Switzerland. This article is an open access article distributed under the terms and conditions of the Creative Commons Attribution (CC BY) license (<https://creativecommons.org/licenses/by/4.0/>).

1. Introduction

SO_x (Sulfur oxides) produced by combustion of fossil fuels in diesel are well known as one of the most significant causes of air pollution [1]. They could directly lead to corrosion as a result, causing acid rains and photochemical smog. More and more stringent regulations for diesel-containing S contents (sulfur) have been established almost worldwide [2]. Therefore, more efforts have been made to maintain sulfur compounds at <10 ppm ("EU Euro V" and "CHN VI") for oil treatments in many countries.

The main drawbacks of traditional HDS are as follows: operating in high temperature and pressure conditions, and using expensive hydrogen. Moreover, the complex heterocyclic compounds, such as dibenzothiophene (DBT), cannot be eliminated easily [3]. Thus, extraction [4], adsorption [5] and ODS [6,7] have been developed in more recent years. ODS for diesel is considered one of the most promising technologies, owing to its high catalytic efficiency for heterocyclic sulfur compounds, its mild operating conditions and its low cost.

Titanium nanotube (TiNT) catalysts have attracted growing attention for ODS for their intrinsic advantages, such as stability, low price, non-toxicity and tunable porosity [8–10]. However, most studies for ODS have used a system with the oil and solid catalysts in a continuous stirred tank reactor (CSTR). A long reaction time (1–2 h) was usually involved in the conversion under certain conditions, causing unsatisfactory atom-efficiency. Therefore, the design of a simple, highly efficient, and recyclable TiNT catalyst for ODS is still to be achieved. A hydrogen-assisted mechanism has been reported to be an important step to increase activation of some intermediates. Very recently, it was reported of hydrogen-assisted catalysts that they gained high activity for C-C coupling reactions over copper [11] and high S removal for ODS over TiO₂ [12,13].

Based on these considerations, together with the fact that H-TiNT is one of the most attractive catalysts for ODS, we attempted to introduce the hydrogen-formed hydrogen-assisted TiO₂ (as well as TiO₂⁺) to the preparation of H-TiNT. The hydrogen-assisted oxidation mechanism over H-TiNT was also explored.

2. Results

2.1. Characterization

2.1.1. X-ray Diffraction

All the samples exhibited several diffraction peaks at $2\theta = 9.7^\circ$, 24.3° , 27.9° and 48.5° , (Figure 1) corresponding to the (100), (110), (310), (020) of $\text{H}_2\text{Ti}_3\text{O}_7$ in TiNTs (JCPDS card 47-0124), respectively. In addition, sample (a) exhibited diffraction peaks at $2\theta = 27.0^\circ$ and 39.1° , corresponding to the (110), (200) crystallographic planes of rutile (JCPDS card 47-0124).

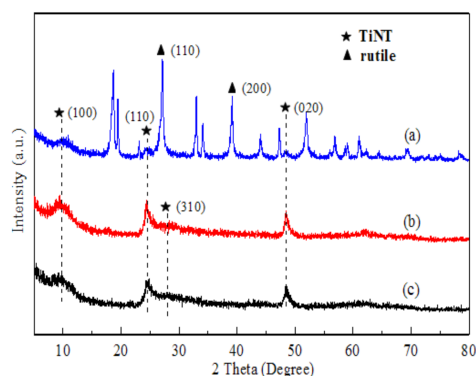


Figure 1. XRD patterns of the catalysts: (a) NT-purchased, (b) NT-P25, (c) NT-TBOT.

2.1.2. FT-IR Spectra

As displayed in Figure 2, the peaks of 473 cm^{-1} , 690 cm^{-1} , 933 cm^{-1} and 1615 cm^{-1} correspond to Ti-O-Ti, O-Na, Ti-O-Na and O-H, respectively, in all the samples. Additionally, the peak band at $750\text{--}980\text{ cm}^{-1}$ (curve (a)) is attributed to the Ti-peroxo species [14,15].

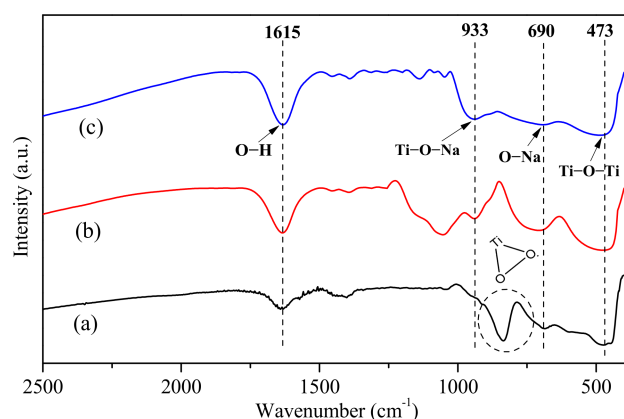


Figure 2. The FT-IR spectra of (a) NT-purchased, (b) NT-P25, (c) NT-TBOT.

2.1.3. SEM

The SEM images of the samples are shown in Figure 3. Unlike Figure 3a, Figure 3b (NT-P25) and Figure 3c (NT-TBOT) illustrate that the products obtained had a morphology similar to that of fibers, with lengths of 200 nm to 1 μm . The tubes in the NT-TBOT sample were distributed uniformly and the length was longer than that in the NT-purchased and NT-P25 samples.

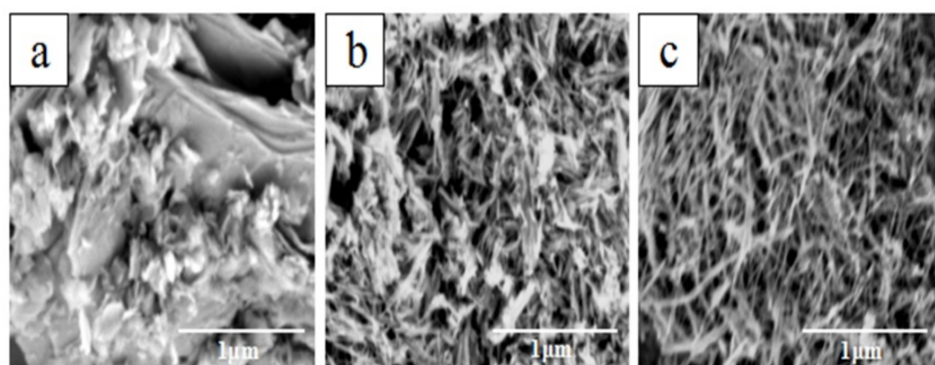


Figure 3. SEM images of the catalysts: (a) NT-purchased, (b) NT-P25, (c) NT-TBOT.

2.1.4. BET Surface Area and Pore Size (Calculated by Nitrogen Adsorption–Desorption)

It can be seen from Figure 4 that all of the samples possessed a typical H3 hysteresis loop, implying the presence of mesopores [16]. However, the hysteresis loop within the range of relative pressure (P/P_0) 0.4–0.99 was quite flat for NT-purchased. Table 1 lists the BET surface areas and the pore size of various catalysts. Among them, the corresponding specific surface area of the catalysts prepared with commercial TiO_2 as the precursor (NT-purchased) was only $45 \text{ m}^2\text{g}^{-1}$, while the specific surface areas of the catalysts NT-P25 and NT-TBOT were significantly increased; these were $245 \text{ m}^2\text{g}^{-1}$ and $283 \text{ m}^2\text{g}^{-1}$, respectively. However, the average pore size distributions of the three catalysts were not much different.

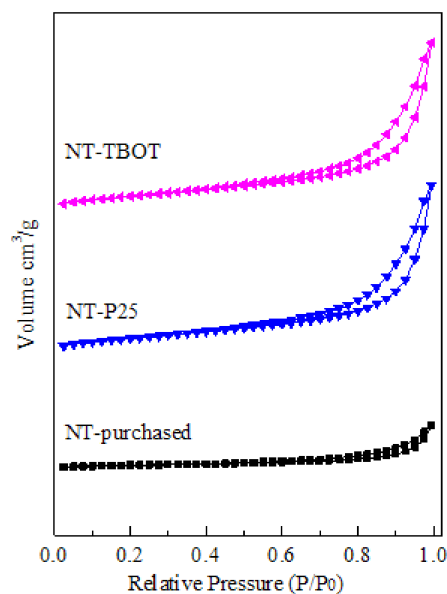


Figure 4. N_2 adsorption–desorption isotherms of catalysts.

Table 1. Physical properties.

Catalysts	S_{BET} (m^2/g)	Pore Size (nm)
NT-purchased	45	3.9
NT-P25	245	3.7
NT-TBOT	283	3.7

2.1.5. UV Analysis

In Figure 5, it was shown that the band gaps of the NT-TBOT and NT-P25 increased distinctly compared to that of the control sample NT-purchased, after being treated with

H_2O_2 . The apparent red shifts at 287 nm and 383 nm were both observed for NT-TBOT + H_2O_2 [17].

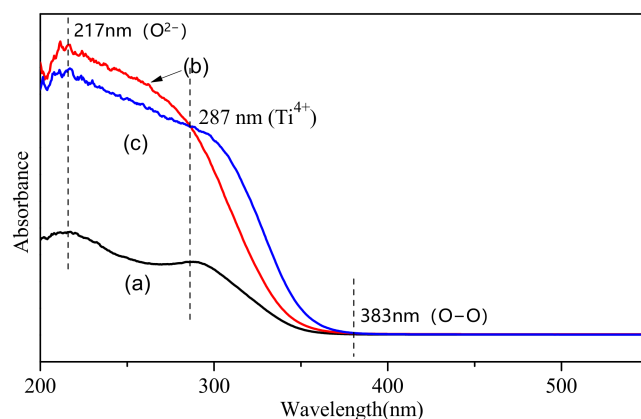


Figure 5. UV-vis spectra of NT-purchased (a), NT-P25 (b), and NT-TBOT (c), after treatment with hydrogen peroxide.

2.1.6. Raman Analysis

The Raman spectra of the samples measured after treatment with H_2O_2 are displayed in Figure 6. Unlike for NT-purchased (mix crystals, see Figure 1), the Raman spectra of NT-P25 and NT-TBOT showed clear bands at 273 cm^{-1} , 459 cm^{-1} , 681 cm^{-1} and 889 cm^{-1} , which correspond to the A1g mode, Ti-O-Ti, Ti-O and O-O (Ti- η^1 -OOH) of the TiNTs phase respectively [18–20].

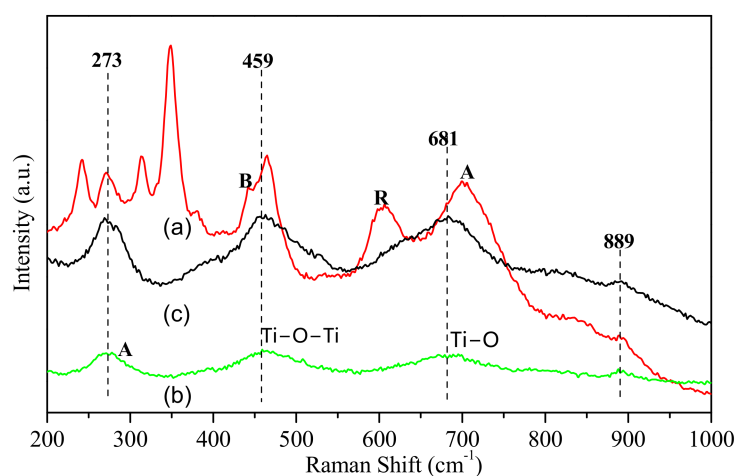


Figure 6. The Raman spectra of NT-purchased (a), NT-P25 (b), and NT-TBOT (c), after treatment with hydrogen peroxide.

2.1.7. NH_3 -TPD

In Figure 7, the two peaks of the low and medium-high temperature range appeared as NH_3 desorption from weak and from medium strength acid sites of the catalyst, respectively. Curve (a) and (b) show a high density of the two kinds of acid sites (with peaks positioned at $159\text{ }^\circ\text{C}$ and $408\text{ }^\circ\text{C}$), which are all higher than those of the NT-purchased sample.

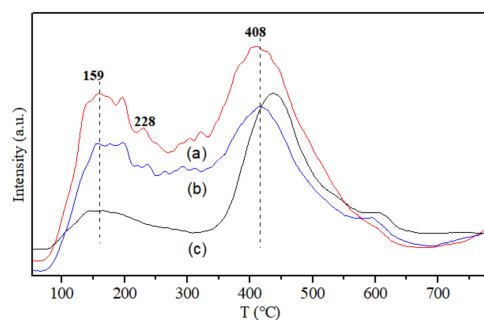


Figure 7. NH_3 -TPD spectra of NT-TBOT (a), NT-P25 (b), and NT-purchased (c), after treatment with hydrogen peroxide.

2.2. Catalytic Performance for ODS

2.2.1. ODS over Titanium Nanotube Catalysts

In Figure 8, it was displayed that no more than 53.0% DBT was removed after half an hour over the NT-purchased sample at the condition of catalyst dosage = 0.1 g, etc., which was listed below Figure 8. In fact, it has been reported that nearly 40% DBT would be displayed in the absence of any catalyst, owing to the liquid–liquid extraction system processes. This maybe attributed to the low purity of the crystal phase, which was proved by XRD in Figure 1. In fact, DBT removal reached 99.9% over NT-TBOT and 88.8% over NT-P25 at the same reaction conditions. The DBT removal over NT-TBOT reached 99.3% in 10 min, which is much higher than the value reached for DBT removal over NT-P25.

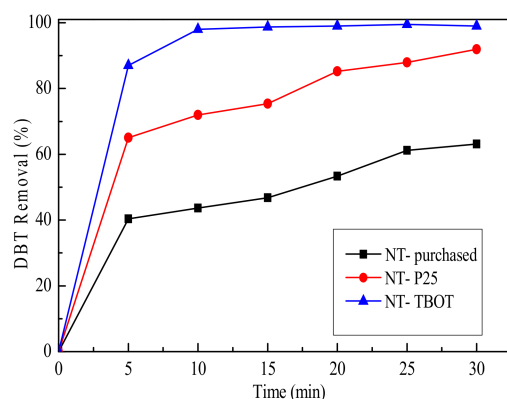


Figure 8. Effects of the different catalysts on the removal of DBT.

Experiment Conditions: catalyst dosage = 0.1 g, temperature of 70 °C, $n(\text{H}_2\text{O}_2)/n(\text{DBT}) = 4$, $V(\text{oil})/V(\text{methanol}) = 1:1$, $C_0 = 320$ ppmw, $t = 30$ min.

2.2.2. Desulfurization for Various Reaction Temperatures

Nearly complete desulfurization efficiency was obtained at all the surveyed temperatures, except at 30 °C for half an hour, as shown in Figure 9. The desulfurization performance was also enhanced with increasing temperature. When the temperature was elevated to 70 °C, the removal of DBT reached the highest level at 10 min. In view of this, the increasing thermal decomposition of H_2O_2 may have occurred under higher temperature [21]. Therefore, the optimal temperature of ODS would be considered to be 70 °C under these reaction conditions.

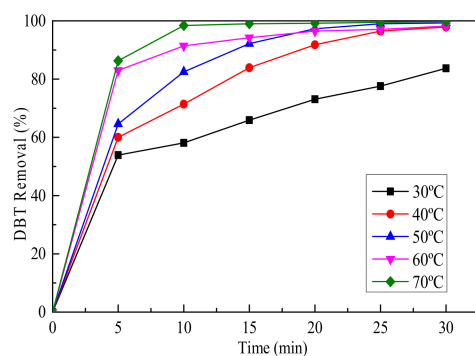


Figure 9. Effects of reaction temperature on removal of DBT.

Experiment conditions: $n(\text{H}_2\text{O}_2)/n(\text{DBT}) = 4$, $V(\text{oil})/V(\text{methanol}) = 1:1$, $t = 30$ min, $C_0 = 320$ ppmw, catalyst dosage = 0.1 g.

2.2.3. Recycling

NT-TBOT was renewed by centrifugation, washed with methanol three times, and dried for 2h in an oven. The DBT removal was only slightly lower than that over the fresh catalyst for the sixth time. Therefore, the catalyst could be recycled no fewer than six times for ODS deeply in Figure 10.

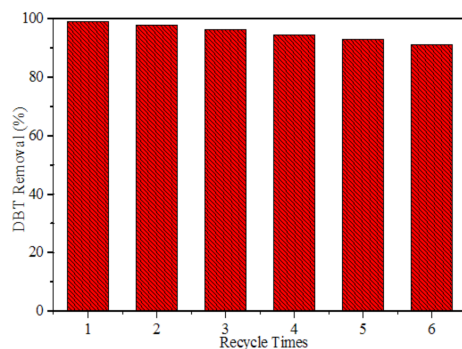
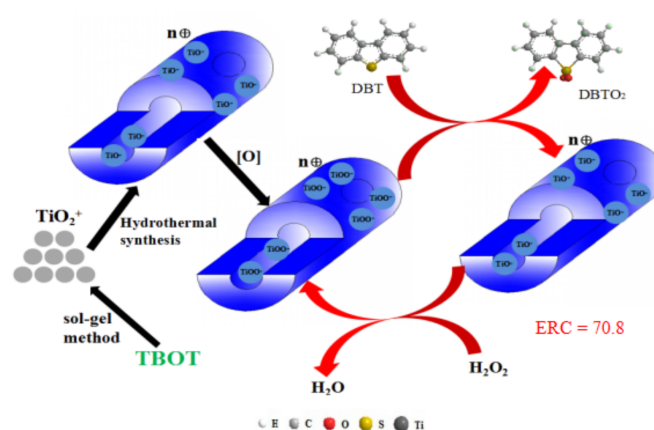


Figure 10. Effects of repeated times of the catalyst on the removal rate of DBT.

Experiment conditions: catalyst dosage = 0.100 g, temperature of 70 °C, $n(\text{H}_2\text{O}_2)/n(\text{DBT}) = 4$, $V(\text{oil})/V(\text{methanol}) = 1:1$, $C_0 = 320$ ppmw, $t = 10$ min.

3. Discussion

An early report revealed that the higher activity over the Ti-containing catalyst for oxidation is partly the result of morphological effects, such as pore size distribution and BET surface [22]. The very similar BET surface areas and pore sizes of NT-TBOT (283 m²/g, 3.7 nm) and NT-P25 (245 m²/g, 3.7 nm) are shown in Table 1. This led to quite a different DBT removal in Figure 8, especially in the first 10 min. Considering that hydrogen-assisted TiO₂⁺ should be a factor in explaining the differences between NT-TBOT and NT-P25 in the mechanism, the proposed mechanism for the catalytic oxidation of DBT by NT-TBOT is shown in Scheme 1. Moreover, this preparation and oxidation process should also be an important chance for obtaining and calculating the amount of [H] over the catalysts.



Scheme 1. The reaction mechanism.

The redox mechanism for Ti-contained catalysis for ODS over TiNT occurs through a mechanism in which Ti^{4+} to Ti^{3+} and Ti^{3+} to Ti^{4+} at the catalytic active site of $Ti-\eta^1-O-O-H$ maintain the catalytic cycle. In other words, Ti^{4+} could be considered as creating four [O] using Ti-O bonds at the active site of TiNT. Therefore, a potential hydrogen-assisted process was taken by molecular-structure modeling to simulate the saturation structure of Ti^{4+} ($Ti-O-O-O-H$, see Scheme S1 in Supplementary Materials). The results confirmed that hydrogen (proton) should be the key factor in increasing the amount of $Ti-O-O-H$ (Ti^{4+}). Additionally, the ionic equilibrium of Na^+ and H^+ usually existed (mol/mol, 1:1) as Na-NT-TBOT (Na-NT-P25) converted into hydrogen form by this process. The Na content was measured to calculate the H content by AAS. Thus, it can be seen in Table 2 that the greatest amount of Na^+ was changed to H^+ by ion exchange over all H-NT. Before the HCl exchange, the Na content of NT-P25 was the highest in Na-NT. (To express our view, saturated sodium content is gained.) Combined with the characterization results of NH_3 -TPD and Py-IR (in Supplementary Materials Figure S1), it is suggested that the Bronsted acid site caused by different H contents of different precursors led to the difference in desulfurization activity. In other words, the TiO_2 -TBOT catalyst itself carries a certain amount of H in the process of synthesizing NT-TBOT and the same amount of H content was retained, so that the content of Na in Na-NT-TBOT is relatively low. After the ion exchange (mol/mol = 1:1) of Na^+ and H^+ was balanced, more content of H remained on the H-NT-TBOT catalyst. In addition, the $Ti-O-O-H$ structure was considered as the catalytic active center, so that there was a certain proportional relationship between H and the active center Ti. Through a literature review, we calculated the value of ERC by using the formula in Table 2. (The active Ti was calculated by the formula in Supplementary Materials Scheme S2). The corresponding ERC was as high as 70.8 over NT-TBOT catalyst.

Table 2. Comparison of Na content and total acidity.

Catalysts	C_{Na^+} ($\mu\text{g/mL}$) Na-NT	C_{Na^+} ($\mu\text{g/mL}$)H- NT	Total Acidity ^a H-NT	Effective Reactant Concentration ^b
NT-P25	82.8	5.0	171.6	66.3
NT-TBOT	36.4	2.6	229.5	70.8

^a measured by NH_3 -TPD. ^b ERC = mol S/mol Ti.

As shown in Supplementary Materials Figure S2, the process consisted of three phases: the catalyst, model oil, methanol and hydrogen peroxide. TiO_2^+ was prepared by hydrothermal synthesis using a procedure adapted from the sol-gel method. The NT-TBOT was prepared using this TiO_2^+ precursor. NT and DBT were extracted to the extractant phase first, and then the active Ti-peroxy species ($Ti-\eta^1-O-O-O$) were formed by reacting with NT and H_2O_2 simultaneously. The Ti-peroxy species passed [O] to the oxidation of

DBT, and the preliminary production DBTO was further oxidized to DBTO₂. Finally, the higher polarity DBTO₂ was retained in the extractant phase, which was separated with fuel.

4. Materials and Methods

Materials: Commercial TiO₂ powder (99%), P25 (Evonik Degussa, Essen, Germany), titanium (IV) tetrabutyl titanate and titanium tetrabutoxide (Jiangtian. Co, Ltd., Tianjin, China, 97%), HCl (Jiangtian. Co, Ltd., 37%), absolute ethanol (Jiangtian. Co, Ltd., 99.8%) and hydrogen peroxide (Jiangtian. Co, Ltd., 30 wt%), and dibenzothiophene (Adamas Reagent, Shanghai, China, 99%).

Methods: Na-NT-TBOT was prepared by a two-step hydrothermal synthesis. First step: The TiO₂ precursor was prepared by hydrolysis of tetrabutyl titanate in acidic media. Second step: The product (nanotube) was followed by hydrothermal treatment for the subsequent hydrothermal crystallization [23,24].

In a typical synthesis, firstly, 4 mL titanium (IV) tetraisopropoxide and 20 mL ethanol were stirred at 25 °C for one hour. A mixture of HCl (4 mL of 0.5 M concentration) and ethanol (10 mL) solution was added. The mixture was stirred for another hour, and then it was transferred to a Teflon-lined stainless-steel autoclave (100 mL), which was heated at 180 °C for 12 h and then cooled down. Afterwards, the solid was filtered, dried at 100 °C for 12 h, and heated in air in a muffle at 5 °C/min up to 350 °C for 2 h to obtain the TiO₂-TBOT precursor. For the second step, 1.0 g of TiO₂-TBOT was mixed with 30 mL of 10M NaOH solution in an autoclave (Newton 2-50, Shanghai LABE Instrument Co., Ltd., Shanghai, China) followed by hydrothermal treatment with stirring at 150 °C for 48 h. The material obtained was filtrated, washed with distilled water, and dried at 60 °C for 24 h. Na-NT-P25 and Na-NT-purchased were synthesized according to the method described in the second step above, using P25 and the commercial TiO₂ powder, respectively.

Na-NT was converted to hydrogen form via conventional ion exchange with HCl (0.1M) at 60 °C, followed by washing and drying. The samples obtained were designated as NT-TBOT, NT-P25 and NT-purchased.

XRD (Bruker D8 Advance) was collected using a Cu Ka radiation source at 40 kV, 40 mA in wide angle (5 to 80°) with a scan rate of 5°/min. FT-IR spectra were recorded by the Nexus 470 (Germany) instrument. SEM was characterized by a Hitachi Limited US-1510 scanning electron microscope. UV-Vis (UV-2550PC) spectra were recorded from 200 nm to 800 nm. The Brunauer–Emmett–Teller (BET, Quantachrome Autosorb-iQ-MP) surface areas were measured at 77 K and calculated by the BJH method using adsorption data. Raman (B&W Tek, Inc., Newark, DE, USA) spectra were collected using a 532 nm laser line. High-resolution continuum source AAS (AA-6300C, Shimadzu, Kyoto, Japan) was selected to determine the content of Na [25]. In a typical NH₃-TPD (Quantachrome) measurement, 0.2 g sample was pre-treatment at 573 K for 1 h in a U-shaped reactor with pure He. Subsequently, the sample adsorbed 10 vol.% NH₃/He at 373 K to saturation, then pure He was used to eliminate the physisorbed ammonia. Finally, the NH₃-TPD analysis was initiated by heating the sample from 323 K to 1073 K at a heating rate of 10 Kmin⁻¹. The amount of evolved ammonia was analyzed by TCD [26]. Please refer to the Supplementary Information (SI) on the catalyst test for the catalytic oxidative desulfurization procedure in model oil [27–29].

5. Conclusions

In conclusion, NT-TBOT (Ti-nanotube, which is prepared from titanium (IV) tetrabutyl titanate) was hydrothermally synthesized from a TiO₂⁺ precursor as the thermo-catalyst for the ODS (oxidative desulfurization) of DBT (dibenzothiophene). NT-TBOT exhibited nearly 100% sulfur removal in 10 min at optimum conditions. DBT in this model oil could be entirely removed using 0.1 g of NT-TBOT catalyst and methanol as the extractant at 343 K in 10 min, while the dosage of the model oil was 15 mL and the O/S (H₂O₂/DBT) molar ratio was 4. The catalysts could be easily regenerated and reused for six cycles.

Furthermore, the hydrogen-assisted thermocatalytic mechanism over NT-TBOT for ODS was also studied.

Supplementary Materials: The following supporting information can be downloaded at: <https://www.mdpi.com/article/10.3390/catal12010029/s1>. Figure S1: The FT-IR spectra of NT-TBOT before pyridine adsorption (a) and after pyridine adsorption (b). Figure S2: Mechanism for the oxidation of DBT by the H-TiNTs. Scheme S1: Molecular structure modeling of active component. Scheme S2: calculation method.

Author Contributions: Methodology and investigation, W.T.; writing—original draft preparation, Y.Y.; writing—review and editing, X.H. All authors have read and agreed to the published version of the manuscript.

Funding: This research was funded by University Scientific Research Project of the Guangzhou Education Bureau, grant number [202032870], the Tianjin College Science & Technology Developing Fund, grant number [2018KJ108] and the Natural Science Foundation of Tianjin grant number, [19JCQNJC04400].

Institutional Review Board Statement: Not applicable.

Informed Consent Statement: Not applicable.

Data Availability Statement: The authors confirm that the data supporting the findings of this study are available within the article [and/or] its supplementary materials.

Acknowledgments: We would like to thank the University Scientific Research Project of the Guangzhou Education Bureau (202032870), the Tianjin College Science & Technology Developing Fund (No.2018KJ108), and the Natural Science Foundation of Tianjin (No. 19JCQNJC04400).

Conflicts of Interest: The authors declare no conflict of interest.

References

1. Zhang, X.G.; Wilson, K.; Lee, A.F. Heterogeneously Catalyzed Hydrothermal Processing of C5–C6 Sugars. *Chem. Rev.* **2016**, *116*, 12328–12368. [[CrossRef](#)] [[PubMed](#)]
2. Yao, Y.; Zuo, M.G.; Shao, P.P.; Huang, X.Q.; Li, J.X.; Duan, Y.S.; Zhou, H.L.; Yan, L.J.; Lu, S.X. Oxidative desulfurization of 4,6-dimethyldibenzothiophene over short titanate nanotubes: A non-classical shape selective catalysis. *J. Porous Mater.* **2020**, *27*, 331–338. [[CrossRef](#)]
3. Zhang, H.; Zhang, Q.; Zhang, L.; Pei, T.T.; Dong, L.; Zhou, P.Y.; Li, C.Q.; Xia, L.X. Acidic polymeric ionic liquids based reduced graphene oxide: An efficient and rewriteable catalyst for oxidative desulfurization. *Chem. Eng. J.* **2018**, *334*, 285–295. [[CrossRef](#)]
4. Seredych, M.; Bandoz, T.J. Template-derived mesoporous carbons with highly dispersed transition metals as media for reactive adsorption of dibenzothiophene. *Langmuir* **2007**, *23*, 6033–6041. [[CrossRef](#)] [[PubMed](#)]
5. Xiao, J.; Song, C.; Ma, X.; Li, Z. Effects of aromatics, diesel additives, nitrogen compounds, and moisture on adsorptive desulfurization of diesel fuel over activated carbon. *Ind. Eng. Chem. Res.* **2007**, *51*, 3436–3443. [[CrossRef](#)]
6. Zuo, M.G.; Huang, X.Q.; Li, J.X.; Chang, Q.; Duan, Y.S.; Yan, L.J.; Xiao, Z.Z.; Mei, S.D.; Lu, S.X.; Yao, Y. Oxidative desulfurization in diesel via a titanium dioxide triggered thermocatalytic mechanism. *Catal. Sci. Technol.* **2019**, *9*, 2923–2930. [[CrossRef](#)]
7. Ma, C.H.; Dai, B.; Xu, C.X.; Liu, P.; Qi, L.L.; Ban, L.L. Deep oxidative desulfurization of model fuel via dielectric barrier discharge plasma oxidation using MnO₂ catalysts and combination of ionic liquid extraction. *Catal. Today* **2013**, *211*, 84–89. [[CrossRef](#)]
8. Lu, S.X.; Zhong, H.; Mo, D.; Hu, Z.; Zhou, H.; Yao, Y. A H-titanate nanotube with superior oxidative desulfurization selectivity. *Green Chem.* **2017**, *19*, 1371–1377. [[CrossRef](#)]
9. Huang, D.; Wang, Y.J.; Cui, Y.C.; Luo, G.S. Direct synthesis of mesoporous TiO₂ and its catalytic performance in DBT oxidative desulfurization. *Microporous Mesoporous Mater.* **2008**, *116*, 378–385. [[CrossRef](#)]
10. Lorencon, E.; Alves, D.C.B.; Krambrock, K.; Avila, E.S. Oxidative desulfurization of dibenzothiophene over titanate nanotubes. *Fuel* **2014**, *132*, 53–61. [[CrossRef](#)]
11. Ma, W.C.; Xie, S.J.; Liu, T.T.; Fan, Q.Y.; Ye, J.Y.; Sun, F.F. Electrocatalytic reduction of CO₂ to ethylene and ethanol through hydrogen-assisted C-C coupling over fluorine-modified copper. *Nat. Catal.* **2020**, *3*, 478–487. [[CrossRef](#)]
12. Ren, X.L.; Miao, G.; Xiao, Z.Y.; Ye, F.Y.; Li, Z.; Wang, H.H.; Xiao, J. Catalytic adsorptive desulfurization of model diesel fuel using TiO₂/SBA-15 under mild conditions. *Fuel* **2016**, *174*, 118–125. [[CrossRef](#)]
13. Wei, Y.; Li, G.; Yi, Y.H.; Liu, J.X.; Guo, H.C. An octane mediated strategy towards Ti-containing HMS-type mesoporous materials incorporated with methyl for high-efficiency oxidative desulfurization. *Fuel* **2020**, *280*, 118660. [[CrossRef](#)]
14. Ohno, T.; Masaki, Y.; Hirayama, S.; Matsumura, M. TiO₂-Photocatalyzed Epoxidation of 1-Decene by H₂O₂ under Visible Light. *J. Catal.* **2001**, *204*, 163–168. [[CrossRef](#)]

15. Liu, Y.J.; Aizawa, M.; Wang, Z.M.; Hatori, H.; Uekawa, N.; Kanoh, H. Comparative examination of titania nanocrystals synthesized by peroxo titanic acid approach from different precursors. *J. Colloid Interface Sci.* **2008**, *322*, 497–504. [[CrossRef](#)]
16. Yao, Y.; Tian, Y.J.; Wu, H.H.; Lu, S.X. Pt-promoted and H β zeolite-supported Ni₂P catalysts for hydroisomerisation of n-heptane. *Fuel Process. Technol.* **2015**, *133*, 146–151. [[CrossRef](#)]
17. Lin, X.H.; Wu, Y.; Xiang, J.; He, D.; Li, S.F. Elucidation of mesopore-organic molecules interactions in mesoporous TiO₂ photocatalysts to improve photocatalytic activity. *Appl. Catal. B Environ.* **2016**, *199*, 64–74. [[CrossRef](#)]
18. Kakihana, M.; Tada, M.; Shiro, M.; Petrykin, V.; Osada, M.; Nakamura, Y. Structure and stability of water soluble (NH₄)₈[Ti₄(C₆H₄O₇)₄(O₂)₄] \cdot 8H₂O. *Inorg. Chem.* **2001**, *40*, 891–894. [[CrossRef](#)]
19. Nag, M.; Ghosh, S.; Rana, R.K.; Manorama, S.V. Controlling Phase, Crystallinity, and Morphology of Titania Nanoparticles with Peroxotitanium Complex: Experimental and Theoretical Insights. *J. Phys. Chem. Lett.* **2010**, *19*, 2881–2885. [[CrossRef](#)]
20. Chaudhuri, M.K.; Das, B. Direct synthesis of alkali-metal and ammonium pentafluoroperoxytitanates(IV), A₃[Ti(O₂)F₅], and first synthesis and structural assessment of alkali-metal and ammonium difluorodiperoxytitanates(IV), A₂[Ti(O₂)₂F₂]. *Inorg. Chem.* **1986**, *25*, 168–170. [[CrossRef](#)]
21. Lu, S.X.; Zhang, H.; Wu, D.; Han, X.; Yao, Y.; Zhang, Q.Z. An Efficient and recyclable polyoxometalate-based hybrid catalyst for heterogeneous deep oxidative desulfurization of dibenzothiophene derivatives with oxygen. *RSC Adv.* **2016**, *6*, 79520–79525. [[CrossRef](#)]
22. Huang, C.Y.; Guo, R.T.; Pan, W.G.; Tang, J.Y.; Zhou, W.G.; Liu, X.Y.; Qin, H.; Jia, P.Y. One-dimension TiO₂ nanostructures with enhanced activity for CO₂ photocatalytic reduction. *Appl. Surf. Sci.* **2019**, *464*, 534–543. [[CrossRef](#)]
23. Cano-Casanova, L.; Amoros-Perez, A.; Ouzzine, M.; Lillo-Rodenas, M.A.; Roman-Martinez, C. One step hydrothermal synthesis of TiO₂ with variable HCl concentration: Detailed characterization and photocatalytic activity in propene oxidation. *Appl. Catal. B* **2018**, *220*, 645–653. [[CrossRef](#)]
24. Kasuga, T.; Hiramatsu, M.; Hoson, A.; Sekino, T.; Niihara, K. Formation of titanium oxide nanotube. *Langmuir* **1998**, *14*, 3160–3163. [[CrossRef](#)]
25. Bi, J.T.; Wang, J.K.; Yang, J.X.; Lu, H.J.; Wang, T.; Huang, X.; Hao, H.X. Double-layered hierarchical titanate and its attaching and splitting mechanism. *Ceram. Int.* **2019**, *9*, 12290–12296. [[CrossRef](#)]
26. Yao, Y.; Zuo, M.G.; Zhou, H.L.; Li, J.Y.; Shao, H.Q.; Jiang, T.; Liao, X.Y.; Lu, S.X. One-Pot Preparation of Ni₂P/ γ -Al₂O₃ Catalyst for Dehydrogenation of Propane to Propylene. *ChemistrySelect* **2018**, *3*, 10532–10536. [[CrossRef](#)]
27. Liao, X.Y.; Wu, D.; Geng, B.Y.; Lu, S.X.; Yao, Y. Deep oxidative desulfurization catalyzed by (NH₄)_xH₄–xPMo₁₁VO₄₀ (x=1, 2, 3, 4) using O₂ as an oxidant. *RSC Adv.* **2017**, *7*, 48454–48460. [[CrossRef](#)]
28. Tian, Y.J.; Yao, Y.; Zhi, Y.H.; Yan, L.J.; Lu, S.X. Combined extraction-oxidation system for oxidative desulfurization (ODS) of a model fuel. *Energy Fuels* **2015**, *29*, 618–625. [[CrossRef](#)]
29. Chica, A.; Corma, A.; Domine, M.E. Catalytic oxidative desulfurization (ODS) of diesel fuel on a continuous fixed-bed reactor. *J. Catal.* **2006**, *242*, 299–308. [[CrossRef](#)]